

DEVELOPMENT OF COMPONENT EXPLOSIVE DAMAGE ASSESSMENT WORKBOOK (CEDAW)

Charles .J. Oswald, Ph.D., P.E.¹
Dale .T. Nebuda, P.E.²

Abstract

This paper summarizes the methods used to develop the Component Explosive Damage Assessment Workbook (CEDAW). The workbook generates pressure-impulse (P-i) diagrams and charge weight-standoff (CW-S) diagrams defining blast loads causing each of four Levels of Protection (LOP) provided by a given structural component. The P-i and CW-S diagrams in CEDAW are generated by “unscaling” scaled P-i curves defining the limits of each LOP in terms of scaled peak blast pressure (Pbar) and scaled positive impulse (Ibar) terms. CEDAW determines P-i diagrams for eleven different common structural component types. CEDAW was developed for the U.S. Army Corps of Engineers Protective Design Center (PDC) by Baker Engineering and Risk Consultants, Inc. (BakerRisk).

The scaling process divides the peak pressure and positive phase impulse of the blast load causing a given non-dimensional dynamic response in a component by properties of that component to obtain generalized Pbar and Ibar terms such that points defined by Pbar and Ibar terms for any number of different blast-loaded components with the same non-dimensional dynamic response will all lie along a single response curve on a scaled P-i diagram. The scaling equations for the various Pbar and Ibar terms used in CEDAW were developed using a conservation of energy approach, where the maximum component response was expressed in terms of a non-dimensional response parameter and the strain energy was based on a response mode (i.e., for response in flexure, tension membrane, arching, etc.) that both depended on the component type. A number of simplifying assumptions were used to reduce the complexity of the scaling equations.

The scaled P-i curves in CEDAW were based on both blast test data and theoretical analyses. Each scaled P-i curve was curve-fit to points defined by Pbar and Ibar from blast loads with a full range of durations that all caused a given non-dimensional response level (i.e., ductility ratio or support rotation) in single-degree-of-freedom (SDOF) analyses of a representative component of each component type. The non-dimensional response levels used in these SDOF analyses were chosen to cause the scaled P-i curves to bound scaled data points with each LOP, which were determined by scaling blast test loads from relevant tests, where the blast loads, component properties, and the damage level were known, with applicable Pbar and Ibar scaling equations. The scaled P-i curves that best defined approximate upper and lower boundaries for scaled data points with each LOP, considering the scatter in the data points, were used as the scaled P-i curves for the given component type in the CEDAW workbook.

¹ Baker Engineering and Risk Consultants, Inc., 3330 Oakwell Court, Suite 100, San Antonio, TX 78218, coswald@bakerrisk.com.

² U.S. Army Corps of Engineers Protective Design Center, 12565 West Center Road, Omaha, NE, dale.nebuda@usace.army.mil.

Introduction

The Facility and Component Explosive Damage Assessment Program (FACEDAP) was developed in the early 1990's to quickly assess blast damage levels to common building structural components using scaled pressure-impulse (P-i) diagrams (Oswald, 1993). The FACEDAP P-i diagrams, and derivatives of these P-i diagrams, have been used in blast assessments of many facilities and have been incorporated into numerous other blast assessment computer tools developed for the U.S. government. The FACEDAP computer program has scaled P-i diagrams for fifteen structural component types with curves that were initially developed theoretically using scaled blast loads from equivalent single-degree-of-freedom (SDOF) analyses that caused given non-dimensional response levels assumed to represent the upper bound of each damage level in representative components. Then, these curves were shifted on the P-i diagrams to better match empirical points for tested structural components with given damage levels defined by scaled the applied blast loads from applicable explosive test data.

Since the development of FACEDAP, more refined SDOF techniques have become available that consider more complex response modes, including tension membrane and arching, such as SBEDS (Nebuda and Oswald, 2004) and considerably more data from structural component response to blast loads has been generated. Also, the importance of the negative phase of the blast load, which limits component response when the peak response occurs after the end of the positive phase of the blast load, is now better understood. Therefore, the PDC contracted BakerRisk to develop the Component Explosive Damage Assessment Workbook (CEDAW) in EXCEL® with updated scaled P-i diagrams classifying component blast damage in terms of the Levels of Protection (LOP) currently used by the U.S. Department of Defense.

Methodology for the CEDAW Workbook

This section presents an overview of the CEDAW methodology. More specific information is presented in the following sections of this paper and elsewhere (Oswald, 2005). The two basic steps in the development of the CEDAW workbook were to: 1) develop scaled P-i diagrams defining scaled blast loads causing each LOP for each of eleven typical component types that are as consistent as possible with both available test data and SDOF-based dynamic analyses, and 2) use these diagrams to quickly generate “unscaled” P-i diagrams in a workbook showing blast loads causing each LOP to a given input component based on unscaling component type-specific scaled P-i diagrams. The workbook also converts the unscaled P-i diagrams into equivalent charge weight-standoff (CW-S) diagrams. These steps involved the following tasks: 1) develop scaling approaches for the blast loads that consider all relevant response modes and non-dimensional response parameters and are as rational and practical as possible, 2) develop curve-fit equations for scaled P-i curves that match the scaled blast load points from SDOF-based dynamic analyses and can be used to quickly “unscale” the curves to show the unscaled blast loads causing each LOP to a given component, 3) obtain as much relevant component blast test data with well defined blast loads, component properties, and blast damage, 4) define descriptions for the component LOP levels and determine the LOP for the available data points based on these descriptions and available post-test photographs and damage descriptions, and 5) use both available test data information and SDOF-based analyses results to generate scaled P-i diagrams that are as consistent as possible with both approaches.

In the first step of the development process, equations that transform the peak pressure and positive phase impulse from the blast load into the scaled blast load terms P_{bar} and I_{bar} , respectively, were developed. The development of these terms is based on conservation of energy equations with consideration of the response modes that affect given component types, including flexure, tension membrane, and arching from axial load, and the non-dimensional response terms that best correlate component response to damage (i.e., ductility ratio or support rotation). Essentially, the P_{bar} and I_{bar} terms must normalize the applied blast load on a component by properties of that component so that two different components with the same non-dimensional response to separate blast loads have the same scaled blast load.

After the equations for P_{bar} and I_{bar} terms were developed, these terms were used to scale the blast loads with a wide range of blast load durations that all cause a given non-dimensional response parameter in SDOF analyses. The P_{bar} and I_{bar} values for each blast load define points on a P-i diagram that can be connected to form a P-i curve. This is illustrated in Figure 1. Each point in the figure, which can be referred to as a scaled SDOF point, represents a scaled blast load causing the given support rotation (θ) and the curve-fits through the points represent scaled P-i curves. The overall figure is a scaled P-i diagram that shows curves of constant response in terms of the scaled peak blast pressure (P_{bar}) and scaled positive blast impulse (I_{bar}) for any component with response that is consistent with the SDOF analyses assumptions and the assumptions used to derive the equations for the P_{bar} and I_{bar} terms.

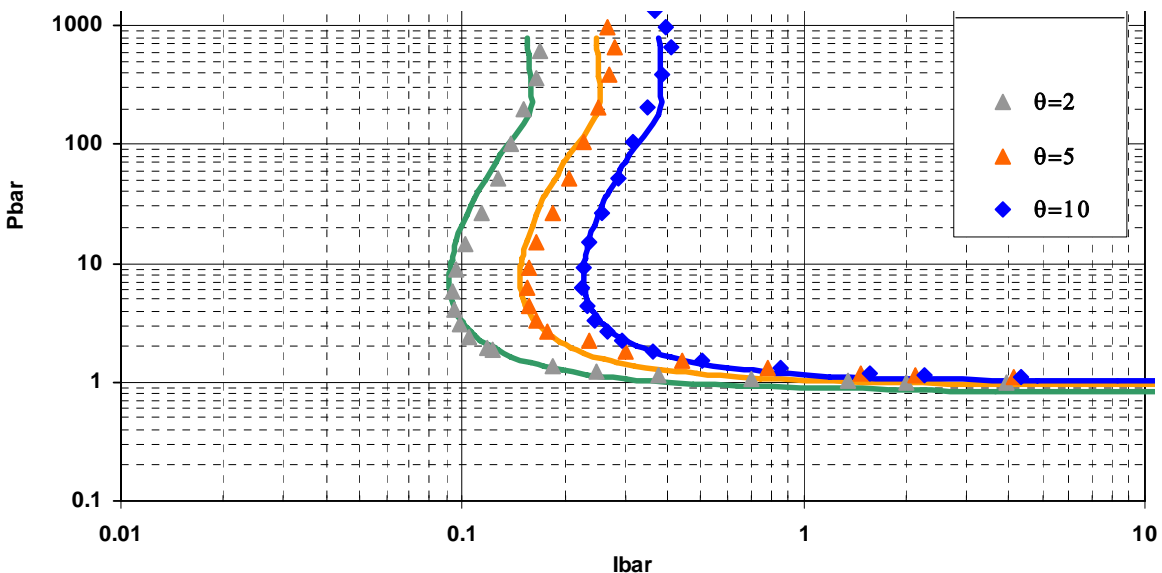


Figure 1. Scaled P-i Curve-fits vs. Scaled SDOF Points in Terms of Support Rotation for Flexural Response of Reinforced Concrete Slabs

Available blast test data on typical structural components with well-defined blast loads, component properties, and blast damage was gathered during the development phase for CEDAW and organized separately based on component type. The blast test data for each component type were characterized in terms of the observed LOP response level, using descriptions for each LOP that were developed in conjunction with the PDC, and the blast loads from the tests were scaled into P_{bar} and I_{bar} values using the appropriate scaling equations. The LOP descriptions are provided in the next section of this paper. The scaled blast loads from the

test data were plotted as points on scaled P-i diagrams for each component type and labeled with the observed LOP in the test. Then, scaled P-i curves, such as those in Figure 1, were developed for each component type using a trial and error approach with different non-dimensional response levels (i.e., different θ values in the case of Figure 1) so that, to the maximum extent possible, all the scaled test points in the regions between the scaled P-i curves all had the same observed LOP. The regions on the scaled P-i diagram between adjacent curves are therefore regions of constant LOP response based on available test data and the non-dimensional response levels used in the SDOF analyses defining these bounding curves are response limits, or response criteria for the LOP.

Scaled P-i curves that created regions of constant LOP response in the available test data for reinforced concrete slabs are illustrated in Figure 2. The curves were generated as described for Figure 1. The data points in Figure 2 were generated by scaling the blast loads from available tests on reinforced concrete slabs that caused the slabs to have LOP as shown in the figure with the same P_{bar} and I_{bar} terms used to scale the blast loads from the SDOF analyses. The SDOF analyses causing the scaled blast loads defining the green, yellow, and blue lines in Figure 2 caused a representative slab to have support rotations of 2, 5, and 10 degrees, respectively. This procedure was used to create scaled P-i diagrams for each of the eleven component types in CEDAW. The SDOF analyses and scaling relationships considered applicable response modes for different component types including flexure, shear, tension membrane, and arching from axial load, as discussed more later in this paper.

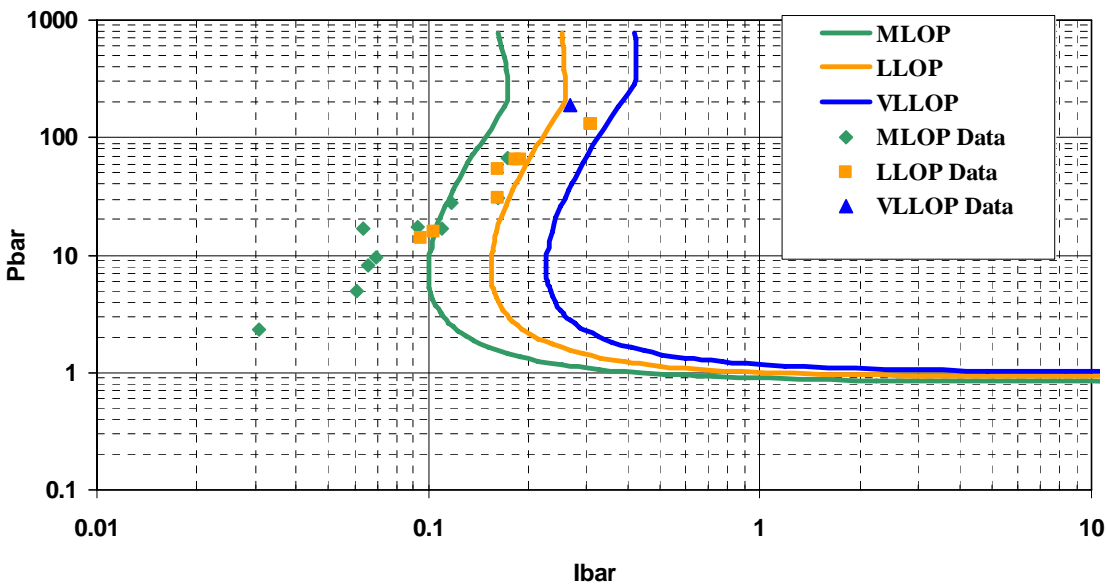


Figure 2. Scaled P-i Curves in Terms of Support Rotation vs. Scaled Data for Reinforced Concrete Slabs

In the final step of the CEDAW methodology, the CEDAW workbook “unscales” the scaled P-i curves for each LOP for the component type matching an input component by using the same P_{bar} and I_{bar} scaling equations used to create the scaled P-i curves in reverse with the properties of the input component. This transforms the scaled curves for the given component type, such as those in Figure 2, which are hard-coded into the CEDAW workbook, into similar curves on an

unscaled P-i diagram, such as the P-i diagram in Figure 3. Since the scaled P-i curves are unscaled using specific properties of the input component, the unscaled P-i diagrams are only applicable for the input component. The unscaled P-i diagram is in terms of peak positive phase pressure and positive phase impulse, instead of P_{bar} and I_{bar} , and the peak positive phase pressure and impulse from a given explosive threat can be used directly in an unscaled P-i diagram to determine the LOP of the input component response. The CEDAW workbook makes this comparison for the reflected and side-on blast loads from an input explosive threat, as shown in Figure 3 for the input charge weight and standoff to the component. The points on the unscaled P-i diagrams are also converted into charge weight-standoff (CW-S) points for a high explosive hemispherical surface burst causing the same peak pressure and positive phase impulse for the side-on and fully reflected conditions. These CW-S points create curves that define the upper and lower boundaries of each LOP for the input component, as shown in Figure 4.

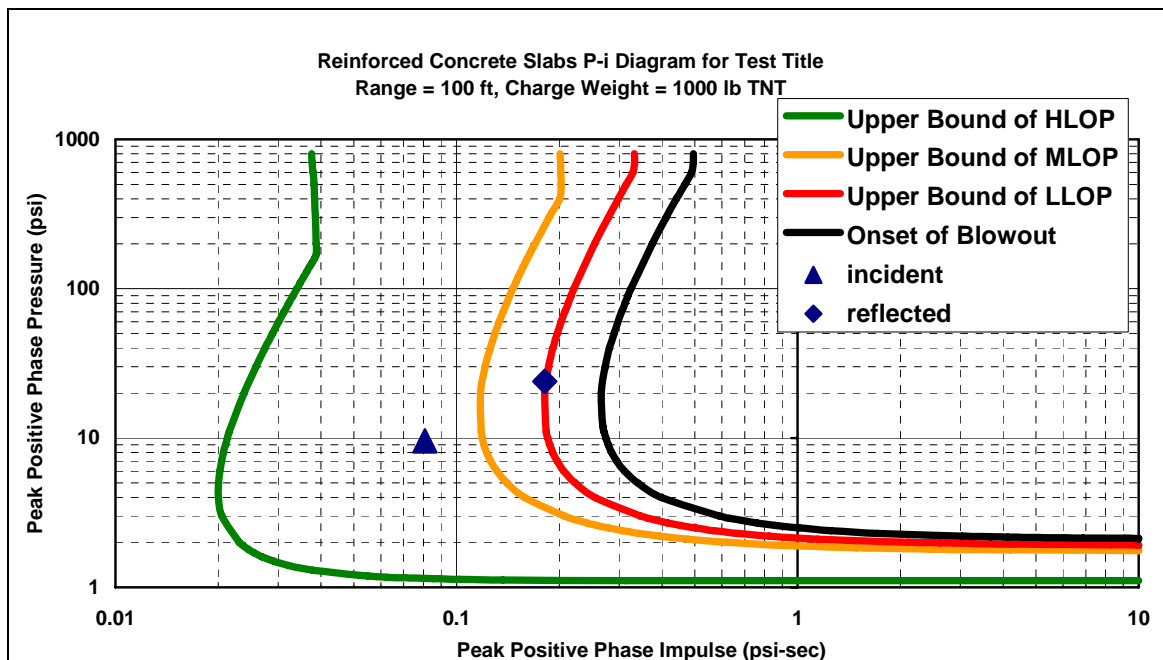


Figure 3. Unscaled P-i Diagram for Specific Input Reinforced Concrete Slab

For a number of component types, there are two sets of scaled P-i curves where one set of curves is for component LOP response defined in terms of ductility ratio, and the other set of curves is for component LOP response defined in terms of support rotations. For other component types, such as reinforced concrete slabs, engineering judgment was used to determine that only one set of scaled P-i curves, based on either support rotation or ductility ratio, was necessary to fully correlate component response at given LOP levels, and therefore LOP response was defined in terms of either ductility ratio or support rotations for these cases. When there are two sets of scaled P-i curves for the component type matching the input component, the CEDAW workbook determines the lower unscaled P-i curve independently for each LOP and plots these unscaled curves on the output unscaled P-i diagram.

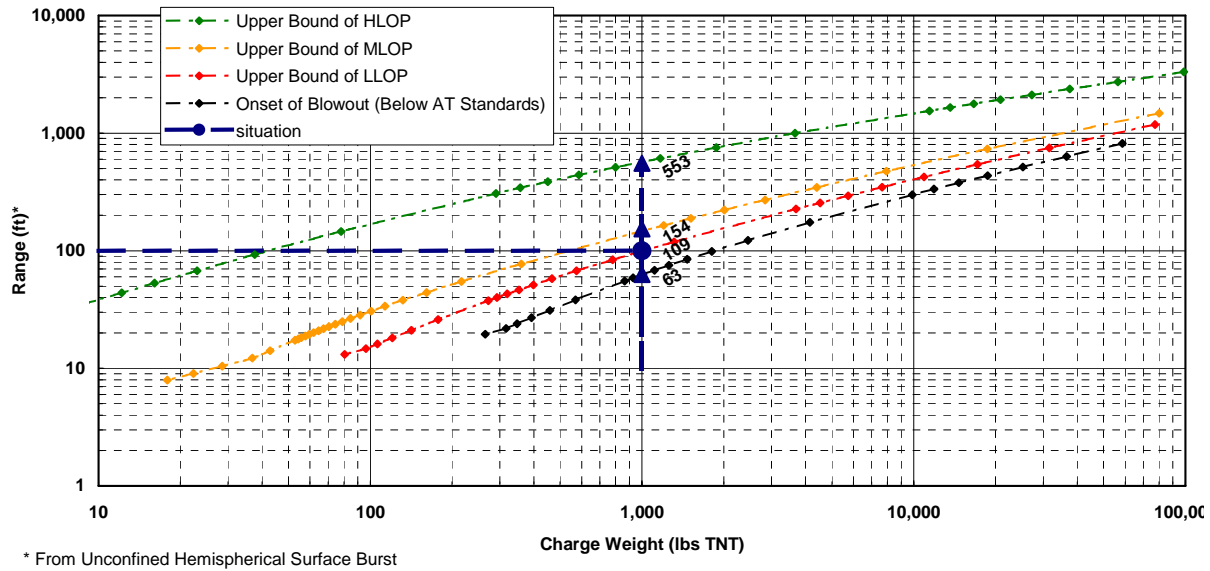


Figure 4. Charge Weight- Standoff Diagram for Reflected Blast Loads on Specific Input Reinforced Concrete Slab

The CEDAW methodology is approximate because of simplifications in the assumptions, derivations, and calculation procedures used to develop the methodology. This includes the use of some simplifying assumptions in the derivation of the blast load scaling equations for the Pbar and Ibar terms that keep the scaling process from becoming too complex, the use of SDOF analyses that make the basic simplifying assumption that only one response mode dominates the component response, and the use of approximate curve-fit equations to develop scaled P-i curves from scaled blast loads points generated with SDOF analyses. Also, the scaled P-i curves are based in part on data where engineering judgment was used to determine the LOP response of the tested components using available photos and damage descriptions and all desired information was not available for all test data. In a relatively few cases, some tested component properties were assumed equal to typically used properties in construction where this was necessary and it was considered a reasonable approach. Test data is shown in detail in the appendices to the final report (Oswald, 2005). These simplifications and assumptions must be considered against the fact that CEDAW is intended primarily for generalized, first-cut type damage assessments and it only predicts response in terms of relatively general, qualitative LOP levels. Also, CEDAW provides very rapid results, which is necessary for damage assessments that must consider a large number of buildings in a short time.

Many comparisons were made to estimate the accuracy of the CEDAW methodology, which are documented in detail elsewhere (Oswald, 2005). Comparisons that the approximate P-i diagrams generated by CEDAW generally match P-i diagrams generated with more exact, and more time-consuming iterative SDOF-based analyses within 5% to 15%. Also, many comparisons of scaled P-i curves developed for different components with the same response mode and response levels showed that these curves, which ideally lie on top of each other, were typically within 10% and were within 30% as a worse case. These comparisons indicate that the assumptions and approximations involved in scaling and unscaling the blast loads and curve-fitting the scaled blast loads used to develop the scaled P-i curves do not typically have a very significant effect on

the final unscaled P-i diagrams generated by CEDAW.

Component Levels of Protection (LOP)

Component LOP definitions were developed in conjunction with the PDC as shown in Table 1, so that available blast test data could be categorized into LOP levels based on the observed response and used to help determine the ductility ratio or support rotation causing the upper and lower bounds of each level of protection (LOP), as described previously and shown in Figure 2. The DoD has issued separate LOP descriptions for overall building damage (DoD, 2003), which were used to help develop the definitions in Table 1. However, components at each LOP do not necessarily cause the overall building to have the same LOP. A separate correlation between component LOP and building LOP, based in part on component type (i.e., is the component a cladding component or a primary framing component) is necessary, but this correlation is outside the scope of this paper.

Curve-Fitting Equations for Scaled P-i Curves

Equation 1 is used in CEDAW as the curve-fit equation for scaled P-i curves for all cases where the scaled P-i points were developed from SDOF analyses that include the effects of negative phase loading. Negative phase loading only affects component response when Pbar is high relative to Ibar, which corresponds to cases where the positive phase blast load durations are relatively short compared to component response time, and causes the curves of scaled SDOF points to bend first to the right, and then to the left at higher Pbar values. The effects of negative phase loads are included for all component types except columns that respond in shear or are subject to connection failure. The parameters A through G in Equation 1 are curve fitting parameters that were varied to cause a curved line that closely fits the scaled SDOF blast loads for given component levels of response representing upper bounds of each LOP, as shown in Figure 1.

Table 1. Component Level of Protection (LOP) Descriptions

Level of Protection	Component Damage
Below AT standards¹ (Blowout)	The component is overwhelmed by the blast load causing failure and debris with significant velocities
Very Low (VLLOP)	A portion of the component has failed, but there are no significant debris velocities.
Low (LLOP)	The component has not failed, but it has significant permanent deflections causing it to be unrepairable. The component is not expected to withstand the same blast load again without failing.
Medium (MLOP)	The component has some permanent deflection. It is generally repairable, if necessary, although replacement may be more economical and aesthetic. The component may be able to withstand the same blast load again without failing.
High (HLOP)	No visible permanent damage
Note 1: This is not an official level of protection. It only defines a realm of more severe structural response that can provide additional useful information in some cases.	

$$I_{bar} = \frac{A(P_{bar})^c}{(\ln[(B)(P_{bar})])^D} \quad \text{for } P_{bar} \leq E$$

$$I_{bar} = (P_{bar} - E)G + F \quad \text{for } P_{bar} > E \quad \text{where } F = \frac{A(E)^c}{(\ln[(B)(E)])^D}$$

Equation 1

where: A, B, C, D, E, F, G = curve fitting parameters

P_{bar} = scaled pressure term applied to component on y-axis of scaled P-i diagram

I_{bar} = scaled impulse term applied to component on x-axis of scaled P-i diagram

In general, the curve-fitting parameters in Equation 1 are only a function of component type and are not a function of component properties. However, Equation 2 shows a special case for the unreinforced masonry wall component type where A and D in Equation 1 are functions of wall properties, including the applied axial load. The equations in Equation 2 were determined by trial and error to cause the curve-fits to match different sets of scaled SDOF points from SDOF analyses where walls had the same response in terms of support rotation but a range of different levels of axial load. This was necessary because of approximations in the derivations of the equations for P_{bar} and I_{bar} for unreinforced masonry walls related to the strain energy absorbed by these components due to arching from axial load after brittle flexural response. This is explained briefly in the next section of this paper and in more detail elsewhere (Oswald, 2005).

$$A(\text{MLOP}) = -0.0096R'^2 + 0.039R' + 0.047$$

$$A(\text{LLOP}) = 1.6 \times A(\text{MLOP})$$

$$A(\text{VLLOP}) = 3 \times A(\text{MLOP})$$

$$D(\text{MLOP}) = -0.47R'^2 + 0.89R' + 0.236$$

$$D(\text{LLOP}) = D(\text{MLOP}) = D(\text{VLLOP})$$

Note: Only applicable for unreinforced masonry walls (see paragraph above)

Equation 2

where: $R' = R_A/R_u$ (ratio of resistance due to arching from axial load divided by resistance from flexure for unreinforced masonry walls)

Equation 3 was used as the curve-fit equation for the scaled P-i curves developed from SDOF analyses that did not include the effects of negative phase loading, which includes the curves for columns in shear response or subject to connection failure. Negative phase blast loads were not considered in the SDOF analyses of column components because these components are typically stiff and strong enough so that their peak response occurs before the end of the positive phase blast load for charge weight-standoff combinations of practical interest. Equation 3 is the curve-fit equation for scaled P-i curves from FACEDAP. The curve-fitting parameters in Equation 1 and Equation 3 for all scaled P-i curves for all component types in CEDAW are documented in the final report describing the development of the CEDAW methodology (Oswald, 2005).

$$Ibar = \frac{0.4 \left(\frac{A}{2} + \frac{B}{2} \right)^C}{Pbar - A} + B$$

Equation 3

where: A, B, C = curve fitting parameters

Derivation of Pbar and Ibar Terms

The equations for the Pbar and Ibar terms in CEDAW vary depending on the assumed response modes for the component and the non-dimensional response term (i.e., ductility ratio or support rotation) used to correlate component response to LOP. Elastic, perfectly plastic flexural response is assumed to be the predominate response mode for all component types in CEDAW except for lightweight steel beams, open web steel joists, columns, and unreinforced masonry walls. Lightweight steel beams and open web steel joists in typical construction may respond with significant tension membrane response at larger deflections, depending on support conditions. The available support restraint in conventional construction is typically not sufficient to develop tension membrane resistance significantly greater than flexural resistance of stronger components, such as most hot-rolled beams, and therefore it is not considered in CEDAW for these component types. Unreinforced masonry components are assumed to respond in brittle flexural response followed by arching action from axial loads, including self-weight. Column components are assumed to have elastic flexural response until the component resistance equals the shear capacity through the cross section (for reinforced concrete columns) or through the connections (steel columns), if the connections control the ultimate component capacity. Limited ductile yielding in shear is then assumed to occur with a resistance equal to the ultimate dynamic shear capacity.

Also, different component types can have LOP that are associated with component response in terms of ductility ratio, support rotation, or both. Therefore, a suite of equations are needed for different Pbar and Ibar terms that are consistent with all the applicable combinations of the response mode and non-dimensional response parameters for the CEDAW component types. Response modes other than those discussed here are possible for all component types in CEDAW. However, the assumption of only these response modes that are considered as predominant for the component types based on blast test data and engineering judgment dramatically simplifies the overall methodology.

Pbar and Ibar Term Equations for Elastic, Perfectly Plastic Flexural Response

Equation 4 and Equation 5 show development of Pbar and Ibar terms for ductile flexural component response. The applied energy from the blast load is described in terms of either work energy for the Pbar equation, or kinetic energy for the Ibar equation, and set equal to the strain energy out to the maximum component deflection for elastic, perfectly plastic flexural response (Baker et al, 1983). The equations are rearranged so that the blast load terms and the maximum structural response term are on opposite sides of the equations in non-dimensional terms and the response term is equal to the ductility ratio or support rotation. The non-dimensional blast load terms with the peak blast pressure in Equation 4 are called Pbar and non-dimensional blast load terms with the impulse in Equation 5 are called Ibar. Both Pbar and Ibar are equal to expressions

that include the non-dimensional response term in Equation 4 and Equation 5, which are valid for the assumptions of these equations that the blast load can be fully expressed in terms of either work energy or kinetic energy. In general, component response to blast load is dependent on both the applied peak pressure and impulse, and therefore both Pbar and Ibar values must be correlated to component response.

$$Px_m = \frac{x_m^2 K}{2} \quad \text{let } \mu = \frac{Kx_m}{R_u} \quad Pbar1 = \frac{P}{R_u} = \frac{\mu}{2} \quad (\text{ductility_based_elastic})$$

$$Px_m = R_u \left(x_m - \frac{x_e}{2} \right) \quad x_e = \frac{R_u}{K} \quad \text{let } \mu = \frac{x_m}{x_e} \quad Pbar1 = \frac{P}{R_u} = 1 - \frac{1}{2\mu} \quad (\text{ductility_based_plastic})$$

Equation 4

$$\frac{i^2}{2K_{LM}m} = \frac{x_m^2 K}{2} \quad \frac{i^2 K}{K_{LM}mR_u^2} = \frac{\mu^2}{2} \quad Ibar1 = \frac{i}{R_u} \sqrt{\frac{K}{K_{LM}m}} = \frac{\mu}{2} \quad (\text{ductility_based_elastic})$$

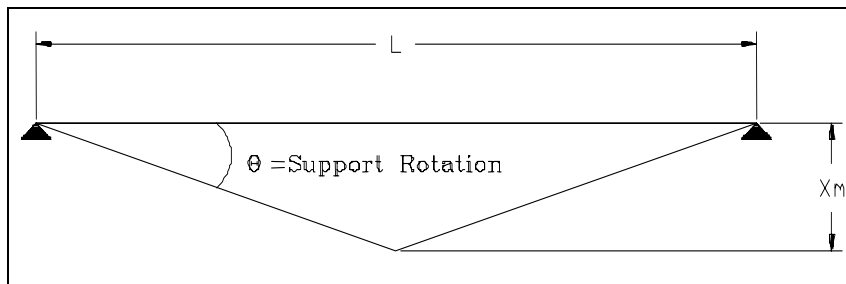
$$\frac{i^2}{2K_{LM}m} = R_u \left(x_m - \frac{x_e}{2} \right) \quad \frac{i^2}{K_{LM}mR_u x_e} = 2\sqrt{\mu-0.5} \quad Ibar1 = \frac{i}{R_u} \sqrt{\frac{K}{K_{LM}m}} = \sqrt{2\mu-1} \quad (\text{ductility_based_plastic})$$

$$\frac{i^2}{2K_{LM}m} = R_u \left(x_m - \frac{x_e}{2} \right) \quad \text{Let } \left(x_m - \frac{x_e}{2} \right) \approx x_m = \theta \frac{L}{2} \quad Ibar2 = i \sqrt{\frac{1}{K_{LM}mR_u L}} = \sqrt{\theta} \quad (\text{SupportRotation_based})$$

Equation 5

where:

- P = peak pressure
- i = applied positive phase impulse
- m = mass of equivalent SDOF system for component
- K_{LM} = load-mass factor of equivalent SDOF system for component
- R_u = ultimate flexural resistance of equivalent SDOF system for component at yield
(ultimate resistance based on shear capacity for reinforced concrete columns and connection shear capacity for steel columns)
- K = flexural stiffness of equivalent SDOF system for component
- x_m = maximum response of equivalent SDOF system for component
- θ = support rotation (radians) – see Figure 5 below
- L = component span length (twice minimum distance from support to yield line for two-way components)
- x_e = maximum deflection of component at ultimate flexural resistance
- μ = ductility ratio, equal to the ratio of maximum deflection divided by the deflection causing yield at all maximum moment locations



$$\theta = \tan^{-1} \left[\frac{2x_m}{L} \right]$$

Figure 5. Support Rotation Angle

The Pbar scaling term in Equation 4 is used to scale the peak blast pressure for component types where LOP correlates best to response in terms of both support rotation and ductility ratio. Either Ibar1 or Ibar2 in Equation 5 is used to scale the positive phase impulse depending on whether scaled P-i curves are developed for response in terms of support rotation or ductility ratio for a given component type. A Pbar term could not be derived for non-dimensional response in terms of support rotation with a simple approximation, such as that used for Ibar2 in Equation 5. However, Pbar is not very sensitive to the response term in general, whether it is based on either term, at ductility ratios greater than 3.0. For example, there is very little change in Pbar1 when ductility ratios of 3 and 10 are substituted into Equation 4. Ductility ratios in the range of 3 or higher are typical for all LOP more severe than HLOP. Therefore, for component types where damage correlates better to support rotation, a Pbar term based on ductility level (i.e., Pbar1 in Equation 4) can be used to scale the peak pressure, and Ibar2 in Equation 5 is used to scale the impulse when the blast loads cause LOP more severe than HLOP.

Pbar and Ibar Term Equations That Include Tension Membrane Response and Brittle Flexural Response With Arching from Axial Loads

Figure 6 shows a simplified resistance-deflection relationship for a component in combined ductile flexure response and tension membrane response that was assumed for the development of Pbar and Ibar equations for this response mode. The tension membrane resistance increases linearly with deflection at the slope K_{TM} in Figure 6 after yielding from in-plane forces occurs in the cross section or in the connection. It is assumed that tension membrane response typically develops relatively slowly with deflection due to support flexibility and slippage in the connections, and response mechanisms in light steel components develop that cause a loss in flexural capacity, such as local compression buckling in the maximum moment region, so that the combined resistance from tension membrane and flexural response does not rise to a value greater than the flexural response until the deflection is greater than the flexural yield deflection.

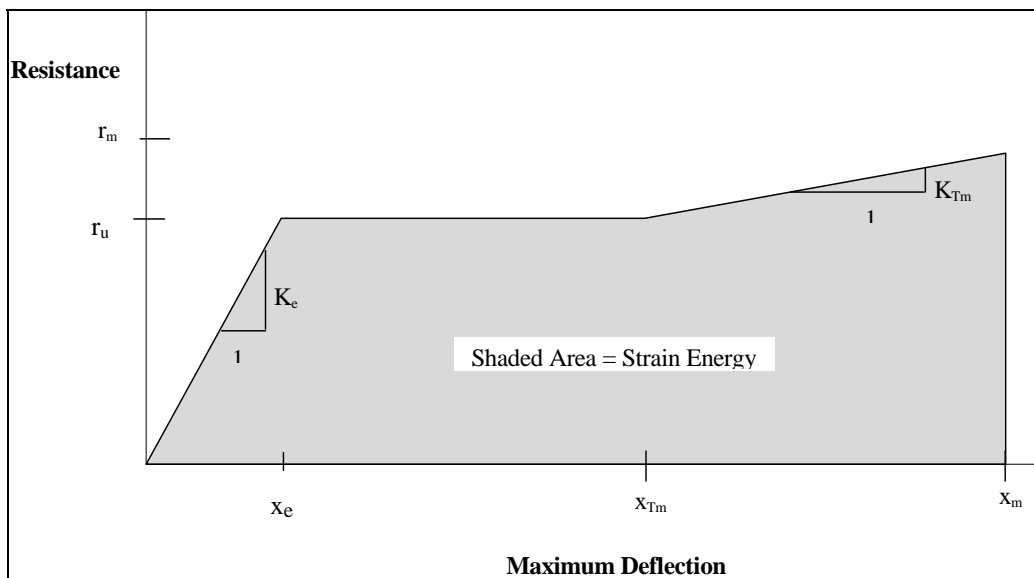
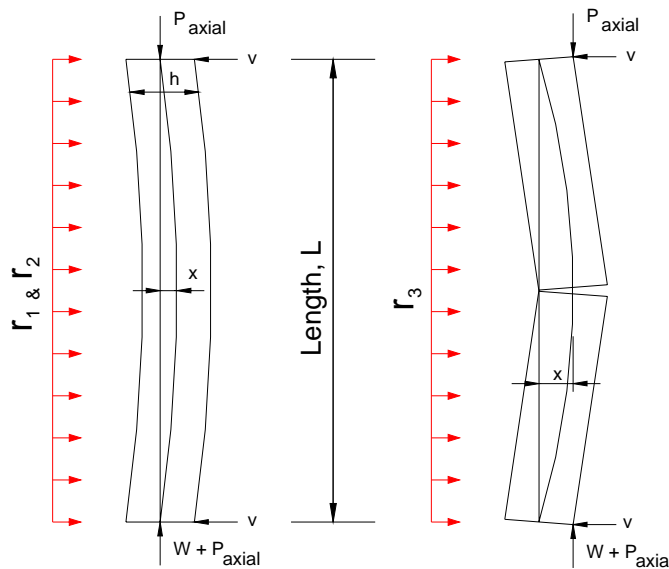


Figure 6. Typical Resistance-Deflection Curve for Component Response with Flexure and Tension Membrane Showing Strain Energy

Figure 7 shows the assumed response mechanism for unreinforced masonry components with brittle flexure response up to the ultimate flexural yield capacity and then post-yield resistance from a arching moment resistance caused by axial load, including the wall self-weight above mid-span. The resisting moment from the axial load has a moment arm equal to the wall thickness minus the wall deflection, as shown in Figure 7. The peak arching resistance from axial load is calculated as shown in Equation 6 and decays to zero when the wall deflection equals the wall thickness. Figure 8 shows the corresponding resistance-deflection relationship. The elastic and elastic-plastic regions are enlarged on the deflection axis for clarity, typically the elastic and elastic-plastic yields occur at very small deflections compared to the wall thickness. This assumed resistance-deflection relationship is largely based on the WAC computer program (Jones, 1989).

For both of these response modes, additional terms are added to the strain energy side of the conservation of energy equations in Equation 4 and Equation 5 that account for additional strain energy from non-flexural response modes. In general, these terms complicate the conservation of energy equation so that a simple, straightforward mathematical solution for a P_{bar} and I_{bar} term are not possible. The conservation of energy equations were simplified so that some parameter ratios in these equations were replaced with constants. The constants were chosen so that P_{bar} and I_{bar} terms based on the simplified energy conservation equations had similar values for different blast-loaded components that had the same non-dimensional response (i.e. support rotation) in SDOF analyses, but different amounts of arching and tension membrane resistance relative to flexural resistance. The derivation of these P_{bar} and I_{bar} terms is discussed in more detail elsewhere (Oswald, 2005).



Response prior to ultimate flexural resistance, r_2 Response after r_2 where $x =$ arching moment arm

Figure 7. Response of Brittle Unreinforced Masonry Wall Under Combined Lateral and Axial Load

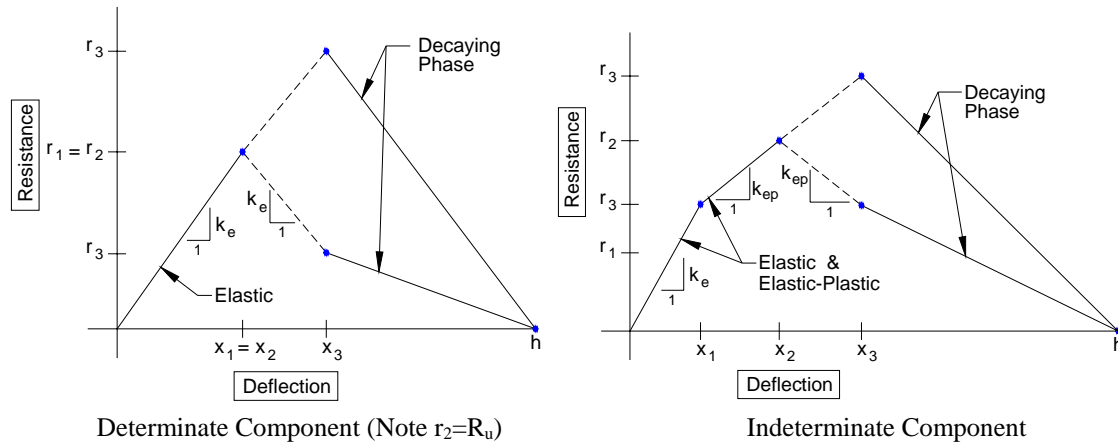


Figure 8. Resistance-Deflection Curves for Unreinforced Masonry with Brittle Flexural Response and Axial Load

$$r_3 = R_A = \frac{8}{L^2}(h - x_2) \left(P + \frac{WL}{2} \right)$$

Equation 6

where:

- r_3 = maximum resistance from axial load effects (also designated as R_A)
- x_2 = flexural yield deflection
- h = overall wall thickness
- P = input axial load per unit width along wall, P_{axial}
- W = area self-weight of wall
- L = wall height

Modifications to Ibar Terms to Scale Negative Phase Load Effects

The Pbar and Ibar terms were derived initially only in terms of the positive phase peak pressure and impulse, even though these terms are intended to predict component response to the entire blast load, including the negative phase. The positive phase blast pressure history from virtually all charge weight-standoff combinations can be approximated as a single shape as required for scaling dynamic response with Pbar and Ibar terms (Baker et al, 1983), equal to a right triangle or exponentially decaying function, depending on the desired accuracy. However, the shape of the blast history including negative phase load is not constant for different charge weight-standoff combinations because of variations in the ratios of peak negative to positive phase pressure, negative to positive phase impulse, and negative to positive phase load durations. This violates the assumption of a constant blast load shape required for scaling with Pbar and Ibar terms.

A suite of SDOF analyses that included negative phase loading was conducted to determine the effect of non-uniformities in blast load shape on analyses where the component resistance, stiffness, and mass were changed separately. In all cases, scaled P-i curves for ductile flexural response of a component with a ductility ratio of 4 were calculated. Ideally, a single scaled P-i curve would be calculated for all cases because the analyses caused the same non-dimensional response with the same assumed response mode. This was true (within some acceptable scatter) only for all the cases where the stiffness and mass was varied. As shown in Figure 9, scaled P-i

curves for cases where the resistance was varied did not lie on top of each other.

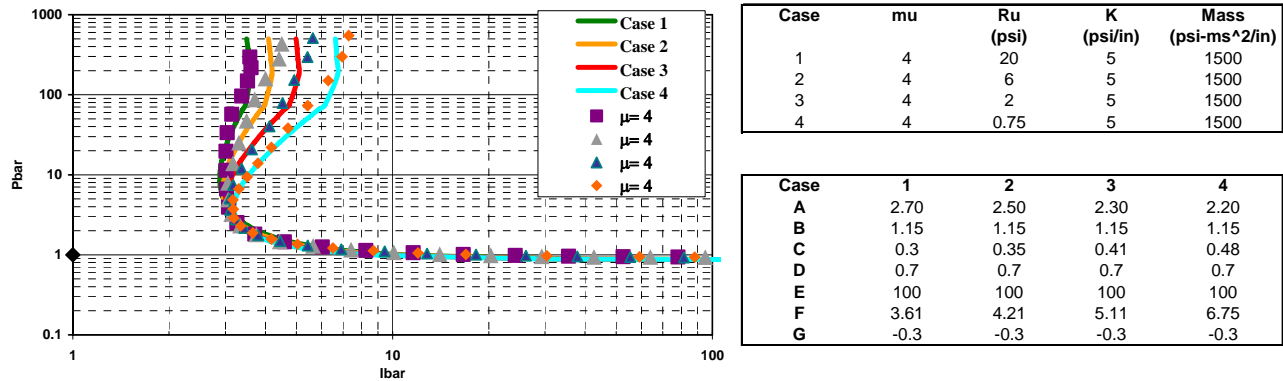


Figure 9. Effect of Ultimate Resistance on Scaled P-i Diagram with Ductility Level of 4

A “first principles” type approach was tried initially to correct this problem, where a net impulse up to the time of maximum response was used in the Ibar term rather than only the positive phase impulse. This did not work well, however, probably because the effect of applied impulse on response prior to the time of peak response is not a simple linear relationship. Rather than trying to go further with first principles approaches, a numerical approach was developed. The effect of resistance on the curve-fitting parameters A through G for Equation 1, as shown in Figure 9, was determined mathematically and this effect was built into the Ibar term so that the effect of resistance on the scaled P-i curves could be accounted for, or scaled, within the Ibar term. Figure 10 shows the same scaled P-i curves from Figure 9 plotted in terms of Ibar1 in Equation 5 with a mathematically determined correction factor Y shown in Equation 7.

As shown in Figure 10, the correction factor does a good job except at very high Pbar values. These very high Pbar values typically correspond to very close-in scaled standoffs where other response modes, such as spalling and localized shear behavior can predominate, and the blast loading over the full component area is very non-uniform. CEDAW is not intended for use in such cases. Similar results were achieved for components with different resistances at different ductility ratios and for cases where the Pbar and Ibar terms were derived based on maximum response in terms of support rotation.

A similar approach was used to derive a different correction factor (Y_{TM}) to account for the effect negative phase blast load on components with differing tension membrane resistance for components with tension membrane. Equation 7 shows all the Pbar and Ibar terms that were developed for the various response modes and response parameters in CEDAW, including applicable correction terms to account for blast load shape changes affecting response at high Pbar values. Note that Pbar is used within the Y and Y_{TM} correction factors since the effect of resistance on the shapes of the P-i curves in Figure 9 increases with Pbar. The Y and Y_{TM} correction factors also include a non-dimensional resistance term, Rbar.

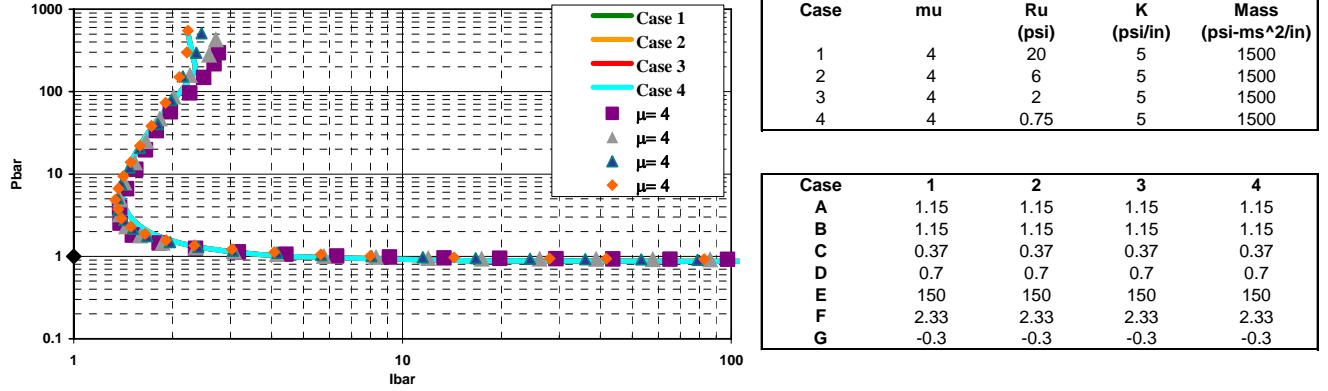


Figure 10. Scaled P-i Diagram with Modified Ibar Term for Multiple Resistances with Ductility of 4

The Pbar and Ibar terms in Equation 7 are used in the CEDAW spreadsheet to determine all scaled P-i diagrams in the CEDAW workbook. The subscripts TM and URM refer to Pbar and Ibar terms for components with tension membrane response and with combined brittle flexure and axial arching response, respectively. These Pbar and Ibar terms can be calculated from the blast load and dynamic structural response parameters for a given structural component and blast load from a given charge weight-standoff combination and used in scaled P-i diagrams to determine the LOP of the component response.

$$Pbar_1 = \frac{P}{R_u} \quad Pbar_{URM} = \frac{P}{R_{MAX}} C_p \quad Pbar_{TM} = \left(\frac{P}{R_u} - 1 \right) \frac{R_u}{K_{TM} L}$$

$$Ibar_1 = \frac{i}{R_u} \sqrt{\frac{K}{K_{LM} m}} Y^* \quad Ibar_2 = i \sqrt{\frac{1}{K_{LM} m R_u L}} Y \quad Ibar_{COL} = \frac{i}{R_u} \sqrt{\frac{K}{K_{LM} m}}$$

$$Ibar_{TM} = \frac{i}{\sqrt{K_{LM} m L R_u}} \left(\frac{R_u}{L K_{TM}} \right)^A Y_{TM} \quad Ibar_{URM} = \frac{i}{\sqrt{K_{LM} m L R_u}} \left(\frac{R_u}{R_A} \right)^B Y$$

where $R_{MAX} = \text{Max}(R_u, R_A)$ $C_p = -0.38R_F^2 - 0.038R_F + 1$ $R_F = \frac{\text{Min}(R_u, R_A)}{R_{MAX}}$

$$Y = \frac{Pbar^{(0.5-0.39Rbar^{-0.127})}}{2.59Rbar^{0.067}} \quad \text{for no tension_membrane_cases except columns in shear}$$

$$Y_{TM} = \frac{Pbar_{TM}^{(0.5-0.19Rbar^{-0.28})}}{1.32Rbar^{0.058}} \quad \text{for tension_membrane}$$

$$Y = 1 \quad \text{for columns_responding_in_shear including connection_failure}$$

$$Rbar = \frac{R_u}{P_a} \quad \text{where } P_a = \text{standard atmospheric pressure}$$

Equation 7

Note: * designates Pbar or Ibar term developed for ductility ratio response term, otherwise all Pbar and Ibar were developed for for support rotation response term

where: x_{TM} = deflection at beginning of tension membrane response (See Figure 6)
 C = ratio of deflection at beginning of tension membrane to maximum deflection ($C \leq 1$)
 B = -0.1 based on trial and error solutions to cause trial and error to cause similar scaled response in impulsive realm for different unreinforced masonry components
 K_{TM} = slope of plastic region of tension membrane response (See Figure 6)
 A = factor determined by trial and error to cause similar scaled tension membrane response in impulsive realm for different components ($A=0.1$ for $R_u > 0.6$ psi, otherwise $A=0.12$)
 R_A = arching resistance from axial load acting through a moment arm based on the wall thickness minus the wall deflection at maximum flexural yielding
See Equation 4 and Equation 5 for definitions of other parameters

Scaled P-i Curves for Each Component Type

Scaled P-i curves were developed for each component type listed in Table 2, based on available test data and results from SDOF analyses that were scaled with applicable $Pbar$ and $Ibar$ terms in Table 2. In all cases, $Pbar1$ and $Ibar1$ from Equation 7 were used to create the scaled P-i curves for HLOP response, since this response level is always assumed to occur at a ductility level of 1.0 as required by the PDC based on their definition of the HLOP response level. The choices of applicable response modes and non-dimensional response parameters for each component type in Table 2 are based on established guidelines such as TM 5-1300, ASCE, and response limits criteria from the PDC, as well as a review of the available test data. When more than one type of response parameter is applicable for a given LOP, the CEDAW workbook plots the P-i curve that causes the LOP to occur at the lowest blast loads, as described previously.

Scaled P-i curves, as shown in Figure 1, were calculated for representative components of each component type using SDOF analyses that considered applicable response modes and non-dimensional response terms from Table 2 and 2% of critical damping. The resistance deflection relationships used in the SDOF analyses were based on elastic, perfectly plastic response without tension membrane or with tension membrane as shown in Figure 6 and brittle flexural response with arching as shown in Figure 8. The representative components had typical properties for each component type, but the exact values of the component properties was not considered critical because the $Pbar$ and $Ibar$ scaling terms generalized the results of the SDOF analyses to be independent of the component properties and geometry.

The blast loads in the SDOF analyses, which included both positive and negative phase loading, were generated by starting with a very small standoff, typically 5 ft, and then increasing the standoff at given intervals and determining the TNT charge weight at each standoff that caused the desired non-dimensional response term value with a goal-searching algorithm. These charge weight-standoff combinations caused blast loads with a full range of load durations that produced the given non-dimensional response term value. Curve-fits from TM 5-1300 (1990) for fully reflected surface burst explosions were used to get positive and negative phase peak pressures and impulses and the positive blast load duration, which defined the beginning of the negative phase load, for each charge weight-standoff combination. The blast load shapes were idealized as linear pressure histories that preserved the positive and negative phase impulse and the beginning time of the negative phase blast loading, as illustrated in Figure 11. The assumed blast load shape had a peak negative phase pressure at the quarter point of the negative phase

duration. Equation 1 or Equation 3 were used to curve-fit the Pbar and Ibar points calculated from the blast loads causing each given non-dimensional response term value.

Table 2. Response Modes, Response Parameter Types, and Pbar and Ibar Terms for Each Component Type in CEDAW

Component Type	Type of Response Parameter	Response Mode	Pbar and Ibar Terms from Equation 7
Reinforced masonry spanning 1-way	Ductility ratio ¹ , support rotation	Elastic-perfectly plastic flexural response	Pbar1, Ibar1 ¹ , Ibar2
Unreinforced masonry spanning 1-way and 2-way		Brittle elastic response and arching based on axial self-weight	Pbar1 ¹ , Ibar1 ¹ , Pbar _{URM} , Ibar _{URM}
Reinforced concrete slab spanning 1-way or 2-way		Elastic-perfectly plastic flexural response	Pbar1, Ibar1 ¹ , Ibar2
Reinforced concrete beam			
Reinforced concrete column	Ductility ratio	Shear response	Pbar1 ² , Ibar _{COL} ²
Hot rolled steel beam	Ductility ratio, support rotation	Elastic-perfectly plastic flexural response	Pbar1, Ibar1, Ibar2
Open web steel joist	Ductility ratio ¹ , support rotation	Elastic-perfectly plastic flexural response with or without tension membrane	Pbar1, Ibar1 ¹ , Ibar2, Pbar _{TM} , Ibar _{TM}
Steel column	Ductility ratio	Connection shear response	Pbar1 ³ , Ibar ³
	Ductility ratio, support rotation	Elastic-perfectly plastic flexural response	Pbar1, Ibar1, Ibar2
Cold-formed steel girts and purlins	Ductility ratio, support rotation	Elastic-perfectly plastic flexural response with or without tension membrane	Pbar1, Ibar1, Ibar2, Pbar _{TM} , Ibar _{TM}
Cold-formed metal stud wall	Ductility ratio	Elastic-perfectly plastic flexural response with and without top connection	Pbar1, Ibar1
Corrugated steel panels and Standing seam steel panels	Ductility ratio, support rotation	Elastic-perfectly plastic flexural response	Pbar1, Ibar1, Ibar2,
Wood beam	Ductility ratio	Elastic-perfectly plastic flexural response	Pbar1, Ibar1
<p>Note 1: Used only for HLOP</p> <p>Note 2: Ultimate resistance in Pbar and Ibar terms using ultimate shear resistance rather than flexural resistance, where the shear capacity includes the dynamic concrete shear strength and shear strength of any closely spaced steel ties.</p> <p>Note 3: Ultimate resistance in Pbar and Ibar terms using ultimate connection shear resistance rather than flexural resistance, where the shear capacity is based on ultimate shear strength of bolted connections.</p>			

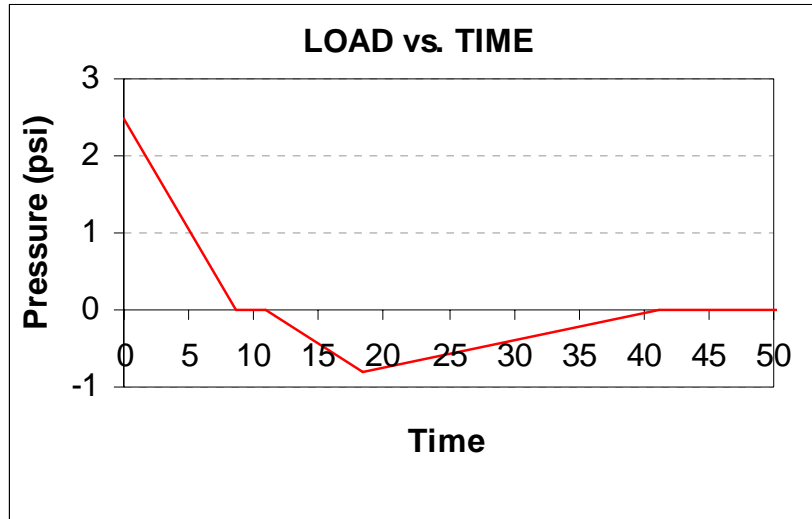


Figure 11. Typical SDOF Analysis Blast Load

Values of the applicable non-dimensional response terms (i.e., ductility ratio and/or support rotation) used in the SDOF analyses were determined using trial and error so that the scaled P-i curves bounded data points from relevant component tests with each observed LOP response level that were scaled in the same manner as the SDOF points, as explained previously. The test data was assigned an LOP based on the component LOP definitions in Table 1. The values of the non-dimensional response terms that caused scaled P-i curves bounding scaled data points with each LOP response level for each component type are referred to as response criteria. For some component types without much available data, the values of the applicable non-dimensional response terms used in the SDOF analyses to create scaled P-i curves bounding each LOP response level were based on published response and design criteria considering the definitions of each LOP in Table 1 (TM 5-1300, 1990), (ASCE, 1997), PDC (2003). The process of determining the response criteria for each component type and LOP is discussed in more detail elsewhere (Oswald, 2005).

Table 3 summarizes the response criteria selected for each LOP and component type. Response criteria in the grey cells were assumed due to a lack of available test data. In all other cases, response criteria were based on available data as described previously and illustrated for corrugated steel panels in the following paragraphs. Column components in Table 3 only have response criteria for the upper bound of LLOP, indicating column failure.

Figure 12 and Figure 13 show corrugated steel panel data scaled using the applicable Pbar and Ibar equations given in Table 2 compared to the scaled P-i curve-fits from SDOF analyses. The response modes indicated in the figures and applicable non-dimensional response term values for each LOP of corrugated steel panels are found in Table 3. The scaled data for each LOP should ideally fall between the upper bound curve for the given LOP and the next curve below and to the left. The scaled data is conservative if it lies above or to the right of the upper bound curve for the given LOP.

Table 3. Response Parameter Criteria for Upper Bound P-i Curves for Each LOP and CEDAW Component Type

Component	Ductility Ratio ³				Support Rotation ³			Support Rotation w/ Tension Membrane ^{1,3}		
	HLOP	MLOP	LLOP	VLLOP	MLOP	LLOP	VLLOP	MLOP	LLOP	VLLOP
One-Way Corrugated Metal Panel	1	3	6	12	3	6	10			
Hot Rolled Steel Beam	1	3	12	25	3	10	20			
Cold-Formed Girt and Purlins ²	1				3	10	20	4	12	20
Metal Stud Connected Top and Bottom	0.5	1	2	3						
Metal Stud Wall Not Connected at Top	0.5	0.8	0.9	1						
Open-Web Steel Joist ²	1				3	6	10	3	6	10
One-Way or Two-Way Reinforced Concrete Slab	1				2	5	10			
Reinforced Concrete Beam	1				2	5	10			
One-Way Reinforced Masonry	1				2	8	15			
One-Way or Two-Way Unreinforced Masonry	1				1.5	4	From data w/o SDOF			
Wood Stud Wall	1	2	3	4						
Reinforced Concrete Column (shear failure)			6							
Steel Column (connection failure)			1							
Steel Column (flexural failure)			4			6				

Note 1: Tension membrane only used in CEDAW when maximum resistance with tension membrane at given support rotation limits is more than 1.27 times ultimate flexural resistance.

Note 2: Support rotation values with tension membrane are used for cold-formed girts/ purlins and open web steel joists except when tension membrane resistance is too low according to Note 1. Even though CEDAW does not explicitly consider tension membrane in this case, limited tension membrane is assumed to allow relatively large support rotations shown in the table.

Note 3: Bold numbers indicate response criteria based on definition of HLOP with an upper bound ductility ratio of 1.0. Bold, shaded numbers indicate component types with a lack of blast data where CEDAW response criteria is based on other available response criteria that is interpreted and used based on LOP component definitions in Table 1. In all other cases, response criteria are based on data.

The data in Figure 12 and Figure 13 is primarily from testing conducted on two-span continuous full-scale steel panels ranging from light 24 gauge panels to heavy 3-inch deep, 20 gauge panels with spans between 4 and 6 ft. Most of the tests were on corrugated steel panels attached to supporting members with self-tapping screws, but the data includes results from several shock tube tests on standing seam panels and insulated steel panels. Most of the data is from a test series conducted for the U.S. Army by ARRADCOM in support of the development of TM 5-1300 for panels supported on rigid frames using high explosive charges. The data also includes shock tube testing of panels supported by lightweight girts and data from a DoD test series on a full-scale pre-engineered building. Detailed test data information and test data references used to develop the response criteria for all component type are documented by Oswald (2005).

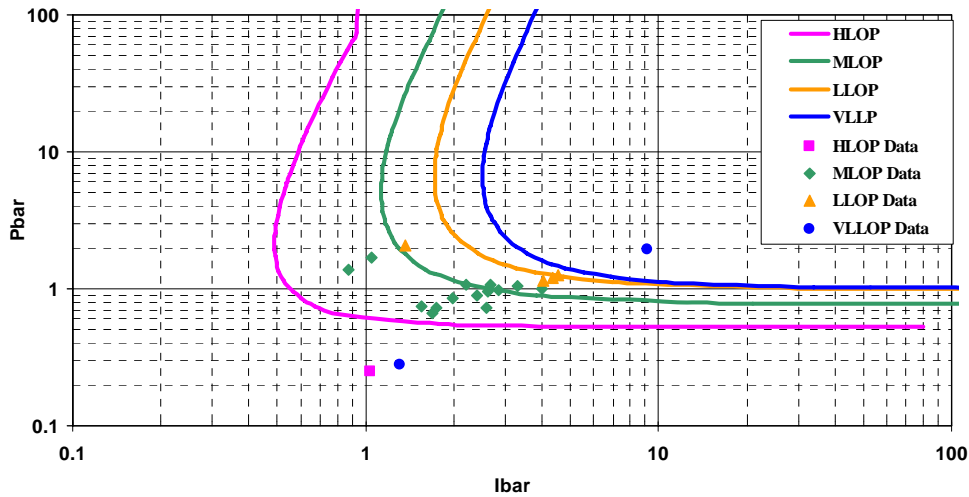


Figure 12. Scaled P-i Curves in Terms of Ductility Ratio vs. Scaled Data for Flexural Response of Corrugated Steel Panels

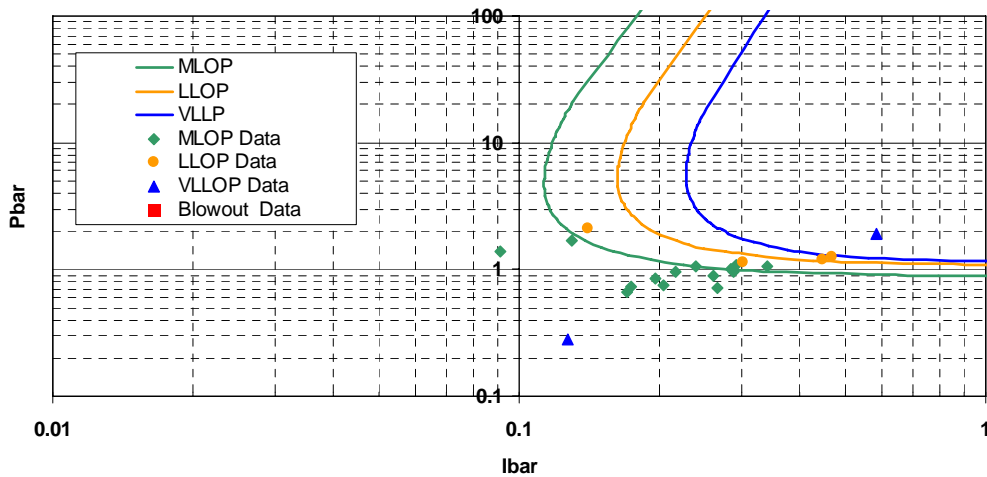


Figure 13. Scaled P-i Curves in Terms of Support Rotation vs. Scaled Data for Flexural Response of Corrugated Steel Panels

Curves similar to Figure 12 and Figure 13 were developed for each component type in Table 2 using the Pbar and Ibar terms shown in Table 2 and the response limits shown in Table 3 (Oswald, 2005). The comparisons shown between the available scaled test data and scaled P-i

curves using the applicable response limits in Table 3 in Figure 12 and Figure 13 are generally representative of similar comparisons for the other component types. The scaled P-i curves based on the response criteria in Table 3 for the input component type are “unscaled” for an input component by the CEDAW workbook, as described previously, and displayed to allow the user to visually determine the component LOP for an input charge weight-standoff combination, as described previously.

Accuracy of CEDAW P-I Curves

The use of the scaled P-i curves in CEDAW to determine the LOP for a blast-loaded component is approximate because of assumptions that fall into three main categories: 1) most of the Pbar and Ibar scaling terms have some simplifying assumptions in their theoretical development; 2) an assumed predominate response mode and non-dimensional response term type (i.e., ductility ratio, support rotation, or both parameters) are assumed to fully account for the dynamic response of each component type; and 3) the scaled P-i curves are based on response criteria in Table 3 that are not well supported by data for some component types or are not consistent with all the available data. It is important to balance these factors against the fact that CEDAW only predicts component response in terms of LOP, which are relatively broad qualitative response regions rather than discrete values, and the fact that CEDAW is intended primarily for quick, initial blast assessments of structural components.

Ideally, scaled P-i curves from the CEDAW methodology that are unscaled for a given component would be identical to P-i curves generated for the same component and response criteria with iterative analyses based directly on the equivalent SDOF system for the component. The SBEDS V2.0 spreadsheet (Nebuda and Oswald, 2004) performs iterative SDOF-based analyses to generate unscaled P-i curves for an input structural component considering the effects of negative phase blast pressures from charge weight-standoff combinations. Response criteria were input into SBEDS equal to the controlling non-dimensional response criteria in Table 3 for HLOP, MLOP, LLOP, and VLLOP response for given components of each component type that were also analyzed with the CEDAW workbook. Comparable unscaled P-i curves for each LOP from SBEDS and CEDAW were compared at three points: 1) the pressure values at the pressure asymptote, 2) the pressure and impulse values at the point of minimum impulse, and 3) the impulse values at the a given high pressure value - typically 100 psi. Comparisons at these three points showed that pressure and impulse values calculated with CEDAW are almost always within 15% of comparable values calculated directly with iterative SDOF-based calculations using SBEDS. The only general trend in the comparisons is for CEDAW to slightly overestimate the pressure value of the minimum impulse point.

Table 4 shows the averages and standard deviations of the ratios of impulses and pressures calculated at comparable points on the P-i curves from comparable CEDAW and SBEDS analyses of twenty-five components covering the full range of component types and response modes. Typically, each component was compared for four different curves, representing HLOP through VLLOP. More details on each compared component are presented elsewhere (Oswald, 2005).

Table 4. Statistical Summary of Comparison of P-i Diagrams Calculated with CEDAW and SDOF Analyses

Statistical Parameter	Pressure Asymptote Comparison	Point of Minimum Impulse Comparison		High Pressure Value Comparison
	Pressure Ratio*	Impulse Ratio*	Pressure Ratio*	Impulse Ratio*
Average	0.98	1.10	1.01	0.99
Standard Deviation	0.09	0.17	0.09	0.08

* Ratio of CEDAW value/SDOF value

Ideally, scaled P-i curves developed from SDOF analyses for different components of the same component type, response mode, and non-dimensional response level should be identical. However, this is not exactly true for the scaled P-i curves used in CEDAW due to simplifications and approximations in the development of the Pbar and Ibar scaling terms. These approximations are most significant for the two most complex response modes, brittle flexure with arching from axial load for unreinforced masonry components and ductile flexure with tension membrane response for light steel components. The Pbar and Ibar equations for these response modes include numerical terms that were back-calculated to cause the scaled P-i curves developed from SDOF analyses for different components with these response modes and identical response levels to be nearly the same. It is very possible that if components with somewhat different properties were used in the back-calculation process, somewhat different values would have been back-calculated for these numerical terms. Also, the effect of different shapes of blast loads causing the same response level in high and low resistance components is approximate.

Comparisons of scaled P-i diagrams were made for each of the different Pbar and Ibar scaling terms in Table 2 using components with a variety of component types, spans, thicknesses, mass, strength and stiffness terms. All scaled P-i curves were generated from SDOF analyses causing applicable non-dimensional response terms in Table 3. These scaled P-i curves were also compared to the applicable scaled P-i curve in CEDAW. The trends noted in similar comparisons for over 50 cases over the full range of component types, response modes, and response parameter types (i.e., ductility ratio or support rotation) are summarized in Table 5. Figure 14 shows a comparison between scaled P-i curves for four steel beam components using the applicable scaling equations from CEDAW and the applicable scaled P-i curve in CEDAW shown in green. This figure is generally representative of comparisons for component types that had Pbar and Ibar scaling equations based on a strain energy equation with only ductile flexural response. Figure 15 shows a comparison between scaled P-i curves for four steel girt components with significant tension membrane response using the scaling equations from CEDAW and the applicable scaled P-i curve in CEDAW shown in green. This figure is generally representative of comparisons for components types that had Pbar and Ibar scaling equations based on a strain energy equation with the two more complex response modes, brittle flexure with arching from axial load for unreinforced masonry components and ductile flexure with tension membrane response for light steel components.

Case	Ductility Ratio	Ru (psi)	K (psi/in)	Mass (psi-ms ² /in)
Case 1	3	11.804	4.3467	1500
Case 2	3	4.8567	2.4839	1500
Case 3	3	2.1585	0.4906	1500
Case 4	3	1.1101	0.1854	1500

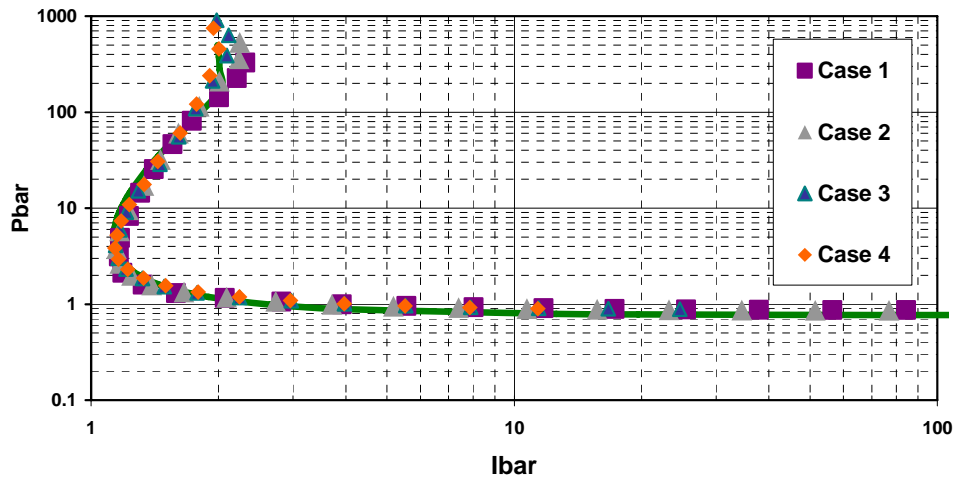


Figure 14. Comparison of Scaled P-i Curves Based on Ductility Ratio for Steel Beams with LOP Response

Case	Support Rotation	Ru (psi)	K (psi/in)	Mass (psi-ms ² /in)	Ktm (psi/in)
Case 1	12	0.2666481	0.0693236	913.4283247	0.0463
Case 2	12	0.5605671	0.2019133	913.4283247	0.0463
Case 3	12	0.9965638	0.6381459	913.4283247	0.0823
Case 4	12	3.7707819	2.8362038	927.3172136	0.3292

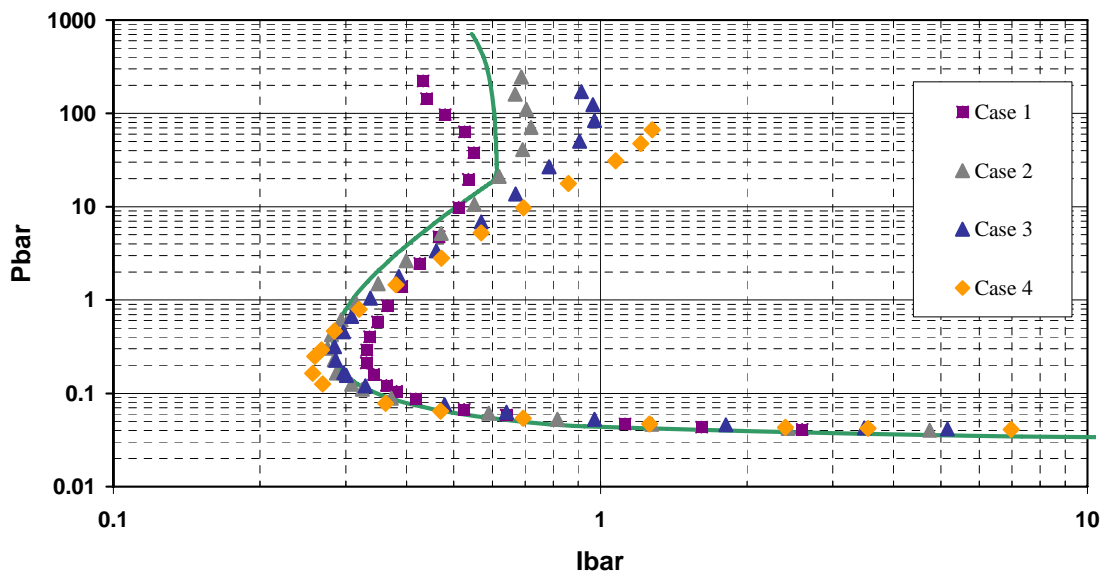


Figure 15. Comparison of Scaled P-i Curves For Cold-formed Beams with Significant Tension Membrane for LLOP Response

Table 5. Trends From Comparisons of Scaled P-i Curves

Response Mode	Response Parameter Type	Comparisons of Scaled P-i Curves for Different Components	Comment
Flexure	Ductility ratio	Very good agreement between scaled P-i curves except minor divergence at very high scaled Pbar values (>100).	Pbar and Ibar equations had no simplifying assumptions. Divergence at high Pbar probably due to dependence of short duration load shape on ultimate resistance (Ru).
Flexure	Support Rotation	Very good agreement between scaled P-i curves except some divergence at very high scaled Pbar values (>100).	Pbar and Ibar equations had only a few assumptions that were very good approximations for higher levels response (i.e., greater than HLOP). Same comment as above for Pbar divergence.
Flexure and tension membrane	Support Rotation	Very good agreement at low Pbar values. Up to 30% divergence in mid Pbar region ($1 < Pbar < 10$) and relatively large divergence in high Pbar region. Selected curve-fit is generally conservative.	Pbar and Ibar equations had significant approximations. The cases of $Pbar < 10$ covers the broad range of practical situations for light gauge steel beams and joists except for small explosions close-in to component (10-30 lbs at less than 20 ft standoff).
Brittle flexure with axial load arching	Support Rotation	Very good agreement for components with $0.7 \text{ psi} < R_U < 2 \text{ psi}$ and wide range of axial load. Up to 30%-40% divergence for significantly higher or lower resistance with axial load, particularly for very large resistance.	Pbar and Ibar equations had significant approximations. However, scaled curve-fits are accurate for cases with most typical ultimate resistance values for one-way and two-way unreinforced masonry walls ($0.5 \text{ psi} < R_U < 2 \text{ psi}$).

Summary and Conclusions

This paper summarizes the methods used to develop the Component Explosive Damage Assessment Workbook (CEDAW). The workbook generates pressure-impulse (P-i) diagrams and charge weight- standoff (CW-S) diagrams defining blast loads causing each of four Levels of Protection (LOP) provided by an input structural component. The workbook generates these diagrams by “unscaling” the scaled P-i curves that define the limits of each LOP for one of eleven different component types. The scaled P-i curves define the full range of scaled blast loads that cause a given LOP in a given component type in terms of scaled peak blast pressure (Pbar) and scaled positive impulse (Ibar). CEDAW calculates P-i and CW-S diagrams for any input component that can be classified as belonging to one of the eleven different common structural component types.

The scaling process divides the peak pressure and positive phase impulse of the blast load causing a given non-dimensional dynamic response in a component by properties of that component to obtain generalized Pbar and Ibar terms so that points defined by Pbar and Ibar terms for any number of different blast-loaded components with the same non-dimensional dynamic response will all lie along a single response curve on a scaled P-i diagram. This is true with an accuracy depending on the assumptions and procedures used to create the scaling equations for the Pbar and Ibar terms. The scaling equations for the various Pbar and Ibar terms used in the CEDAW scaled P-i diagrams were developed using a conservation of energy

approach, where the maximum component response was expressed in terms of a non-dimensional response parameter and the strain energy was based on a response mode (i.e., for response in flexure, tension membrane, arching, etc.) that both depended on the component type. A number of simplifying assumptions were used to reduce the complexity of the scaling equations.

The scaled P-i curves in CEDAW were based on both blast test data and theoretical analyses. Each scaled P-i curve was curve-fit to points defined by P_{bar} and I_{bar} from blast loads with a full range of durations that all caused a given non-dimensional response level (i.e., ductility ratio or support rotation) in single-degree-of-freedom (SDOF) analyses of a representative component of each component type. The non-dimensional response levels used in these SDOF analyses were chosen to cause the scaled P-i curves to bound scaled data points with each LOP, which were determined by scaling blast test loads from relevant tests, where the blast loads, component properties, and the damage level were known, with applicable P_{bar} and I_{bar} scaling equations. The scaled P-i curves that best defined approximate upper and lower boundaries for scaled data points with each LOP, considering the scatter in the data points, were used as the scaled P-i curves for the given component type in the CEDAW workbook. The non-dimensional response levels for these selected scaled P-i curves are the response limits for each LOP of the component type.

The accuracy of P-i curves generated with CEDAW was assessed in two studies. First, P-i curves generated with the CEDAW spreadsheet were compared to P-i curves generated with iterative SDOF-based analyses for the same component and response criteria for twenty-five components covering the full range of component types and response modes. Ideally, these P-i curves should match exactly. The pressure and impulse values calculated with CEDAW were almost always within 15% of comparable values calculated directly with iterative SDOF-based calculations. The only general trend in the comparisons was for CEDAW to slightly overestimate the pressure value of the minimum impulse point on the P-i curves.

Also, the scaled P-i curves used in CEDAW were compared to scaled P-i curves generated using SDOF-based analyses of arbitrary components of the applicable component type using the same P_{bar} and I_{bar} scaling equations as CEDAW and the applicable response criteria from CEDAW. The generated scaled P-i curves should ideally match the applicable scaled P-i curves in CEDAW. This was not always true due to simplifications and approximations in the development of the P_{bar} and I_{bar} scaling terms. These approximations are most significant for the two most complex response modes, brittle flexure with arching from axial load for unreinforced masonry components and ductile flexure with tension membrane response for light steel components. The scaled P-i curves generated with SDOF-based analyses for over 50 components with a full range of component types, response modes, and applicable response parameter types (i.e., ductility ratio or support rotation) generally matched the applicable scaled P-i curves in CEDAW generally within 10% for component types with flexural response modes, which comprise most of the component types, and within approximately 35% at worst for blast loads at typical standoffs for component types with the two more complex response modes.

References

ASCE Task Committee on Blast Resistant Design, *Design of Blast Resistant Buildings in Petrochemical Facilities*, American Society of Civil Engineers, N.Y., N.Y., 1997.

Departments of the Army, the Navy and the Air Force, *Structures to Resist the Effects of Accidental Explosions*, Department of the Army Technical Manual TM 5-1300, Department of the Navy Publication NAVFAC P-397, Department of the Air Force Manual AFM 88-22, November 1990.

Department of the Army, "*Design and Analysis of Hardened Structures to Conventional Weapons Effects* (DAHS CWE)," Army Technical Manual TM 5-855-1, November 1997.

"DoD Minimum Antiterrorism Standards for Buildings," United Facilities Criteria (UFC) 4-010-01, October 8, 2003.

Johnston, B. G., "*Damage to Commercial and Industrial Buildings Exposed to Nuclear Effects*," Federal Civil Defense Administration, Report WT-1189, February, 1956.

Jones, Patricia, "*WAC: An Analysis Program for Dynamic Loading on Masonry and Reinforced Concrete Walls*," Submitted to Faculty of Mississippi State University in Partial Fulfillment of the Requirement for the Degree of Master of Science in the Department of Civil Engineering, December, 1989.

Nebuda, D. and Oswald, C.J., "SBEDS (Single degree of freedom Blast Effects Design Spreadsheets)," Proceedings from the 31st DoD Explosives Safety Seminar, San Antonio, Texas, August, 2004.

Oswald, C.J., "*Facility And Component Explosive Damage Assessment Program (FACEDAP) User's Manual*," Prepared by Southwest Research Institute for the Department of the Army, Corps of Engineers, Omaha District, CEMRO-ED-ST, Contract No. DACA 45-91-D-0019, April, 1993.

Oswald, C.J., "Component Explosive Damage Assessment Workbook (CEDAW)," Prepared by Baker Engineering and Risk Consultants for the U.S. Army Corps of Engineers Protective Design Center, Contract No. DACA45-01-D-0007-0013, May, 2005.

Response Limits Summary Sheet, Working document of the U.S. Army Corps of Engineers Protective Design Center (PDC), September, 2003.

Stea, W., Dobbs, N., Weissman, S., Price, P., and Caltagirone, J., "*Blast Capacity Evaluation of Pre-Engineered Building*," US Army Armament Research and Development Command, Weapon Systems Laboratory, Contractor Report ARLCD-CR-79004, March, 1979.

Stea, W., Sock, F.E. and Caltagirone, J., "*Blast-Resistant Capacities of Cold-Formed Steel Panels*," US Army Armament Research and Development Command, Weapon Systems Laboratory, Contractor Report ARLCD-CR-81001, May 1981.